



Transport spectroscopy of NS nanowire junctions with Majorana fermions

Elsa Prada,¹ Pablo San-Jose,² and Ramón Aguado¹

¹*Instituto de Ciencia de Materiales de Madrid (ICMM-CSIC), Cantoblanco, 28049 Madrid, Spain*

²*Instituto de Estructura de la Materia (IEM-CSIC), Serrano 123, 28006 Madrid, Spain*

(Received 29 March 2012; revised manuscript received 26 October 2012; published 12 November 2012)

We investigate transport through normal-superconductor nanowire junctions in the presence of spin-orbit coupling and magnetic field. As the Zeeman field crosses the critical bulk value B_c of the topological transition, a Majorana bound state (MBS) is formed, giving rise to a sharp zero-bias anomaly (ZBA) in the tunneling differential conductance. We identify novel features beyond this picture in wires with inhomogeneous depletion, such as the appearance of two MBSs inside a long depleted region for $B < B_c$. The resulting ZBA is in most cases weakly split and may coexist with Andreev bound states near zero energy. The ZBA may appear without evidence of a topological gap closing. This latter aspect is more evident in the multiband case and stems from a smooth pinch-off barrier. Most of these features are in qualitative agreement with recent experiments [V. Mourik *et al.*, *Science* **336**, 1003 (2012)]. We also discuss the rich phenomenology of the problem in other regimes which remain experimentally unexplored.

DOI: 10.1103/PhysRevB.86.180503

PACS number(s): 74.45.+c, 03.65.Vf, 71.10.Pm, 73.21.Hb

Following early ideas based on exotic p -wave superconductors,^{1,2} it has been recently predicted that Majorana quasiparticles should appear in topological insulators³ and semiconductors with strong spin-orbit (SO) coupling.^{4–8} In proximity to s -wave superconductors, these systems behave as topological superconductors (TSs) when the excitation gap is closed and reopened again: as the gap crosses zero, Majorana bound states (MBSs) appear wherever the system interfaces with a nontopological insulator (see Refs. 9 and 10 for reviews).

The TS transition occurs when an external Zeeman field B exceeds a critical value $B_c \equiv \sqrt{\mu^2 + \Delta^2}$ defined in terms of the Fermi energy μ and the induced s -wave pairing Δ .^{7,8} This prediction has spurred a great deal of experimental activity towards detecting MBSs in hybrid superconductor-semiconductor systems. Indeed, signatures of Majorana detection have been recently reported in Ref. 11. These experiments (and subsequently Refs. 12 and 13) clearly show the emergence of a zero-bias anomaly (ZBA) in differential conductance dI/dV measurements as B increases. It has been predicted that such a ZBA reflects tunneling into the MBS.^{14–16} Crucially, the emerging ZBA, which signals the TS transition, should be accompanied by a closing and reopening of the excitation gap.^{17,18} something which is, however, *not* observed. Other experimental findings, such as ZBA splitting and coexistence of Andreev bound states (ABSs) and MBSs,¹¹ also need further analysis.

Motivated by this, we present here a detailed study of transport through normal-superconductor (NS) junctions containing topological wires. As in the experiment, the wires are tunnel-coupled to the normal reservoir by a pinch-off gate V_p (to allow for transport spectroscopy using dI/dV), and are depleted by an additional gate V_d in order to bring B_c down to accessible fields (since the induced potential U_d lowers the Fermi energy $\mu \rightarrow \mu - U_d$). The depletion profile, however, is necessarily *inhomogeneous*, since it cannot extend deep into the superconducting side due to efficient screening, see Fig. 1 and Ref. 11. We find that for this class of devices, a number of distinct transport regimes arise as the various sections of the

wire transition to different electronic phases. We characterize these regimes and the rich phenomenology that results beyond the simplest picture.^{14–16} In particular, we address the question of whether the ZBAs are related to Majorana physics, and confirm that this is indeed the case for long depletion regions. We also analyze the development of ABSs close to zero energy when the pinch-off gate lies at a finite distance from the NS junction. Our main results are summarized in Fig. 4(e) where we demonstrate that the dI/dV of realistic junctions with inhomogeneous depletion and multisubband filling *may not* show a distinct closing of the gap and yet exhibit ZBAs of Majorana origin. In most cases, these ZBAs show a residual splitting and may coexist with ABSs, features also observed in Ref. 11.

Model. We first consider a one-dimensional NS junction [see Fig. 1(a)], with a BCS-type Hamiltonian $H = H_0 + H_{\text{pairing}}$, where

$$H_0 = \int dx \psi^\dagger(x) \left[\frac{-\partial_x^2}{2m} + i\alpha\sigma_y\partial_x + B\sigma_z + U(x) - \mu \right] \psi(x)$$

$$\text{and } H_{\text{pairing}} = \int dx \psi^\dagger(x) i\Delta(x)\sigma_y\psi^\dagger(x) + \text{H.c.}$$

Here α is the SO coupling and B is the Zeeman splitting (given by $B = g\mu_B\mathcal{B}/2$, where \mathcal{B} is an in-plane magnetic field, μ_B is the Bohr magneton, and g is the nanowire g factor). We assume a position-dependent pairing $\Delta(x)$ induced by the superconducting electrode such that $\Delta(x \rightarrow \infty) = \Delta$ and $\Delta(x \rightarrow -\infty) = 0$. The term $U(x) = U_d(x) + U_p(x)$ is composed of two parts: $U_p(x)$ comes from the pinch-off gate V_p in the normal region at a distance L_N from the NS interface, and $U_d(x)$ models the potential induced by the depletion gate V_d .¹⁹ Gate V_d may extend all the way into the normal side of the NS interface [case N^dS^dS , with a depleted length $L_d = L_{N^d} + L_{S^d}$, Fig. 1(a)], or be limited to the end of the superconducting side [case NS^dS , $L_d = L_{S^d}$, Fig. 1(b)]. We will consider the former case first, where we cover different parametric regimes, and then turn to the second one, which is closer to the experimental setup.¹¹ Realistic experimental parameters are $\Delta = 250 \mu\text{eV}$ is the induced gap that, for an InSb effective mass $m = 0.015m_e$, corresponds to

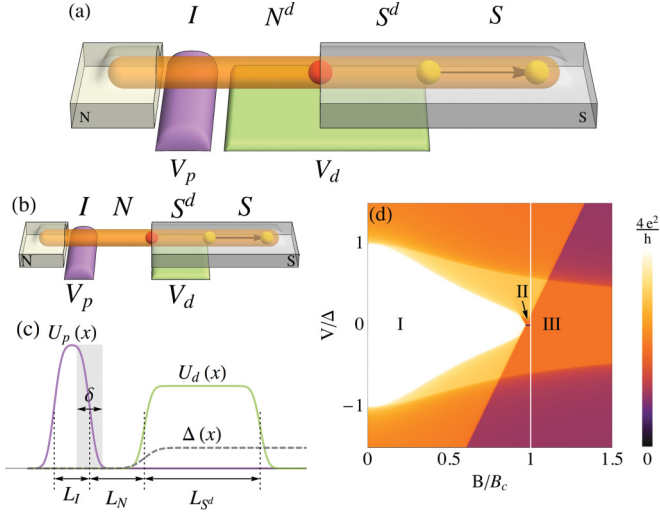


FIG. 1. (Color online) Schematics of the nanowire junction in the $N^d S^d S$ (a) and $NS^d S$ (b) setups, and spatial variation of superconducting gap and potential profiles (c). Gate V_d depletes the wire, while V_p creates a tunnel contact (I) to the left (normal) reservoir. One (red) or two (red and yellow spheres) Majorana bound states may appear at the edges of the depleted region depending on the Zeeman field and gate voltage V_d . (d) Transport regimes for a transparent NS junction ($V_{d,p} = 0$, $\mu = 4\Delta$) in the Zeeman-field-bias plane.

a length scale $L_\Delta \equiv \hbar/\sqrt{m\Delta} \equiv 142$ nm. Strong SO coupling, representative of InSb wires,²⁰ is $\alpha = 20$ meV nm, with SO length $L_{SO} = \hbar^2/(m\alpha) = 200$ nm $= 1.4L_\Delta$.²¹

Scales. A localized MBS is formed at the boundary of a trivially gapped and a TS portion of the wire. At a point x the wire will be in the TS phase if $\Delta(x) > 0$ and

$$B > \sqrt{[\mu - U(x)]^2 + \Delta(x)^2}. \quad (1)$$

The asymptotic value of the critical field is the proper (bulk) critical field B_c . Apart from B_c , several other Zeeman scales dictate the junction's transport properties. The first one is the TS critical field in the depleted part of the superconducting wire, $B_c^d \equiv \sqrt{(\mu - U_d)^2 + \Delta^2}$, which is smaller than B_c , as is the purpose of the depletion gate. It should be noted, however, that the depleted S^d region has a *finite* length, which crucially affects Majorana modes for $B_c^d < B < B_c$, as discussed later, while the S portion is assumed infinite. Second, there is the field above which the normal side of the wire becomes a helical liquid (momentum and spin become correlated). In the $NS^d S$ case (normal side not depleted), this is $B_h \equiv \mu$, which is typically slightly smaller than B_c , but bigger than both B_c^d and the corresponding helical field in the $N^d S^d S$ case, namely, $B_h^d \equiv |\mu - U_d| < B_c^d$. Finally, there is the superconducting gap itself, $B_\Delta \equiv \Delta$, whose significance will become clear later. All these scales (B_Δ plus $B_c^d < B_h < B_c$ in the $NS^d S$ case, or $B_h^d < B_c^d < B_c$ in the $N^d S^d S$), control different aspects of the junction's differential conductance in the B - V plane.

Differential conductance. The dI/dV of a NS junction may be related to the intrinsic conductance at zero temperature by the expression²²

$$\frac{dI(V)}{dV} = \frac{e^2}{h} [\mathcal{N} - \text{Tr}(r_{ee}^\dagger r_{ee}) + \text{Tr}(r_{eh}^\dagger r_{eh})]_{\epsilon=V}.$$

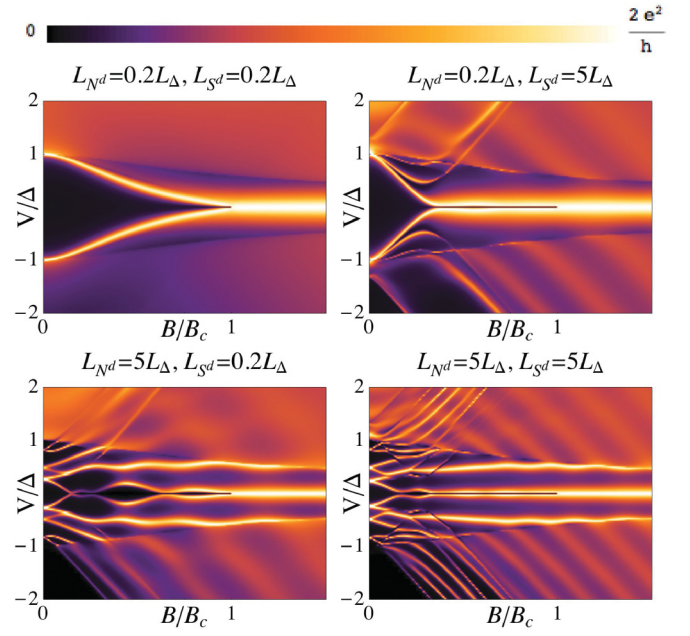


FIG. 2. (Color online) Density plots of the dI/dV in the $N^d S^d S$ junction ($\mu = 4\Delta$, $U_d = 3.25\Delta$, $U_p = 25\Delta$, $\delta = 0$) for $L_{SO} = 1.4L_\Delta$ as a function of bias voltage V and Zeeman field B with a tunnel pinch-off barrier and a depletion region of length $L_{N^d} + L_{S^d}$, Fig. 1(a). Different columns feature increasing values of L_{S^d} from left to right, whereas different rows feature increasing length L_{N^d} from top to bottom.

Here, \mathcal{N} is the number of propagating channels in the normal side at energy $\epsilon = V$, and r_{ee} and r_{eh} are their normal and Andreev reflection matrices. These matrices can be computed in a number of ways. The most flexible is the recursive Nambu Green's function approach, employed here (for full details, see Ref. 23).

Before considering the effect of $U(x)$, we show the transport phase diagram [see Fig. 1(c)] in the simple NS transparent limit, i.e., in a regime where the concepts of MBSs and ZBAs no longer hold. We observe different transport regions in the B - V plane characterized by an integer $dI/dV \approx ne^2/h$, with $n = 0, 1, 2, 3, 4$. Such is the case of Cooper pair transport (region I, $n = 4$) or single quasiparticle transport (region III, $n = 2$). The latter is a TS regime, whose topology becomes evident in the dI/dV despite the fact that the associated Majorana fermion is completely smeared out due to the gapless spectrum for $x < 0$.²⁴⁻²⁷ Between these two regions, the helical regime is characterized by a fully suppressed zero-bias conductance (region II, $n = 0$). These results extend the concept of half-integer conductance quantization²⁴ beyond linear response.

We now consider the $N^d S^d S$ junction with the full $U(x)$. Its dI/dV response (with $L_{SO} = 1.4L_\Delta$) is plotted in Fig. 2. Different panels cover different ratios L_{N^d}/L_Δ and L_{S^d}/L_Δ . The tunnel barrier U_p is tuned in each case to yield spectroscopic resolution in the transport response. A wide range of behaviors becomes apparent, which reflects the local density of states (DOS) at the pinch-off gate. The most paradigmatic one is probably the one in the top-left panel. It reflects the closing of the effective superconducting gap (marked by the gap-edge

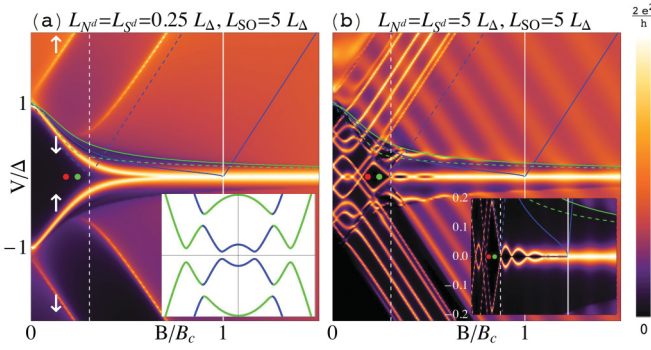


FIG. 3. (Color online) dI/dV in a short (a) and long (b) $N^d S^d S$ junction ($\mu = 4\Delta$, $U_d = 3.25\Delta$, $U_p = 22\Delta$, $\delta = 0$). Colored guide-lines represent the gap at large (green) and small (blue) momentum (see band structure in the left inset) in the depleted (dashed) and bulk (solid) superconducting regions. Vertical solid (dashed) line marks B_c (B_c^d). (a) For short depletion region, a minigap transport regime is developed for $B > B_\Delta$ (green dot), unrelated to Majorana modes. (b) Long depletion region, however, allows the existence of ABSs around zero energy below B_h^d (red dot) and (split) Majorana fermions for $B < B_c$, see blowup in the right inset.

conductance peaks) as B increases. The gap-edge DOS peak transforms into a Majorana mode at zero energy for $B > B_c$ [pictured in Fig. 1(a) as a red sphere]. The gap reopens in the TS phase (see solid blue line in Fig. 3), but the local DOS at the contact is no longer peaked because the spectral weight is transferred to the Majorana mode. Hence, a prototypical three-pronged structure arises in the B - V plane. However, the relevant phenomenology is by no means exhausted by this. Different scenarios arise at large L_{N^d} (Fig. 2, bottom row), with the development of ABSs, or large L_{S^d} (right column), with the development of ZBAs below B_c . Further phenomenology is obtained by varying L_{SO} .²³

Short $N^d S^d S$ junction. We now analyze in more detail the short junction case, $L_{N^d}, L_{S^d} \ll L_\Delta$ (top-left panel in Fig. 2). The scale B_c^d has little meaning in this case, since any pair of Majorana modes forming at the ends of a short TS wire will strongly hybridize into two conventional states with energies $\sim \pm\Delta$. The effect of increasing L_{SO} is to flatten the gap-edge dI/dV peak (bright yellow) to lower energies, as shown in Fig. 3(a) ($L_{SO} = 5L_\Delta$). At these large L_{SO} , spin becomes a good quantum number and the Zeeman field splits the particle and hole bands of the S region into spin-up and spin-down subbands (white arrows in Fig. 3). Particle and hole gap edges anticross at zero energy for $B > B_\Delta$ (green dot), resulting in a minigap (which vanishes for $L_{SO} \rightarrow \infty$) with almost flat edges near zero. This structure appears as a (split) ZBA below B_c that is unrelated to Majorana mode formation.²⁸

Long $N^d S^d S$ junction. Increasing the length L_{N^d} of the depleted normal wire gives rise to ABSs in the N^d region that are probed by the tunnel barrier U_p (see bottom row of Fig. 2). Increasing L_{SO} we find these ABS resonances approaching a degenerate zero energy crossing, see Fig. 3(b). These low-energy ABSs, however, cease after the helical transition at B_h^d (red dot). While the ABSs move up and down in energy for $B < B_h^d$ depending on their spin character, as soon as the N^d region becomes helical, all ABSs disperse away from zero energy with increasing B , since incoming states do not

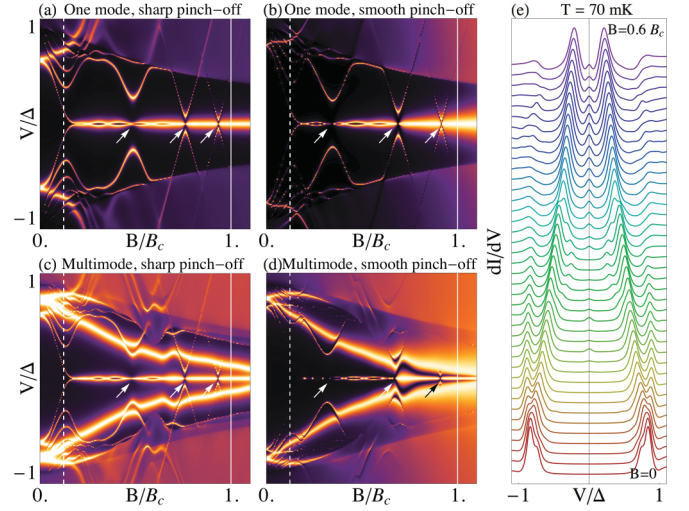


FIG. 4. (Color online) dI/dV response at zero temperature of an $NS^d S$ junction similar to that of Ref. 11, for one open (spinful) mode (a,b) and two modes (c,d). ABSs coexist and suppress (white arrows) the ZBA from Majorana pairs within the depletion region. For increasing smoothness of the pinch-off profile $U_p(x)$ (b and d), the local gap-edge peak is washed out, leaving an isolated ZBA at $B < B_c$ without a visible closing of a transport gap. Vertical guidelines and color scale as in Fig. 3. (e) Finite temperature dI/dV version of (d). Different curves are shifted for clarity from $B = 0$ (bottom) to $B = 0.6B_c$ in 40 steps. Parameters: $\mu = U_d = 8\Delta$, $U_p \sim 20$ - 30Δ , $L_N = 450$ nm, $L_S^d = 1$ μ m, $\delta = 100$ nm, and $B_c^d = 0.12B_c$.

have spin partners anymore. Beyond the second threshold B_c^d (vertical dashed white line), the local band gap closes in the S^d region (dashed blue line) and a ZBA builds up, which is caused by Majorana fermion pairs forming in the S^d region of length L_{S^d} , also assumed large. The finite L_{S^d} , however, produces a residual splitting of the two Majoranas, visible in the ZBA that oscillates with B (Refs. 29–32) as long as $B < B_c$. Above the bulk B_c , the rightmost Majorana escapes to $x \rightarrow \infty$ (see Fig. 1), where it no longer overlaps with the one at the $N^d S^d$ interface, and the splitting vanishes [see inset of Fig. 3(b)].

$NS^d S$ junction. We now turn to the type of setup explored in Ref. 11, the $NS^d S$ case. The crucial difference with the $N^d S^d S$ setup is that the ABSs zero-energy anticrossings may coexist with Majorana ZBAs in the S^d region, since the N region becomes helical *after* the S^d region becomes topological. When that happens, the zero-energy ABSs repel the MBS wave function (usually delocalized into the N region) back into the S^d region, hence decoupling it from the lead. As a result, the ZBA, as measured by the dI/dV , is suppressed (see arrows in Fig. 4, where $L_{SO} = 1.4L_\Delta$). In a single-mode wire (Fig. 4, top row), this may happen only for $B < B_h < B_c$, since it requires an interface between a nonhelical N and a topological S^d .³³ Interestingly, the above behavior agrees with the experimental observation of an intermittent ZBA that disappears and reappears as an ABS anticrosses at zero energy. Constant- B sweeps of U_d are also found to closely correlate with the experiment.²³

A further feature apparent in the experiments is the absence of gap-edge singularities closing just before the formation of the ZBA. Up till now, all potential profiles have been

assumed spatially abrupt [decay length $\delta = 0$ in all profiles of Fig. 1(c)]. Imperfect screening, however, will lead to gate-induced potentials that decay slowly along the wire, specially at low electron densities. When a smooth $U_p(x)$ profile is taken into account, the gap-edge peaks are quickly washed out, and the dI/dV in the tunneling regime is no longer a perfect measure of the local density of states.³⁴ Unlike for sharp pinch-off barriers, transmission through smooth barriers mostly preserves longitudinal momentum. Since moreover barrier transmission is lower for smaller momenta, the gap-edge resonance closing around zero momentum at B_c^d is poorly probed by a smooth barrier. Visibility is restored as B increases beyond B_c^d , since then the Zeeman splitting increases the momentum components of all resonances, including the ZBA. Figure 4(b) shows this effect. Note on the other hand that the gap-edge signal at higher energies $\sim \Delta$ is roughly constant in B . This corresponds to the large-momentum band edge, not the true gap edge at small momentum. The former band edge shows no sign of the different transitions (the TS transition at B_c in particular), and never closes. Therefore, all zero-energy structure appears disconnected from any closing of the gap, as measured by the dI/dV .

Transport features connected to large momenta should be *enhanced* in multisubband systems. The pinch-off condition for tunneling spectroscopy requires a higher U_p barrier in this case to shut off the additional open modes, which will necessarily contribute with a stronger signal relative to the shallower, lower momentum mode. This is likely the experimental situation in Ref. 11, where the observed gap-edge signal exceeds the amplitude of the ZBA. To confirm this idea, we performed multisubband transport simulations (see implementation details in Ref. 23). In Figs. 4(c) and 4(d), we show results corresponding to a fixed μ defined from the bottom of the topmost subband, which becomes topological at low magnetic fields, while the lower ones remain trivial. The single-mode analysis carries over unchanged, albeit with a stronger gap edge and the associated high-momentum structure of the additional modes. Figure 4(e) shows constant B traces of Fig. 4(d) at finite temperature ($k_B T = 70$ mK). Thermal smearing washes out the ZBA splitting, while also reducing its height.

Conclusions. We have identified various transport regimes in depleted NS nanowire junctions with SO coupling and Zeeman field. Depending on the Zeeman field, the wire as a whole may be in any given combination of helical/nonhelical and trivial/topological phases for its normal and supercon-

ducting portions, respectively. These include *helical depletion* ($B_h^d < B < B_c^d$) and *topological depletion* ($B_c^d < B < B_h, B_c$) phases that arise at fields below those of the proper *helical bulk* ($B_h < B < B_c$) and *topological bulk* ($B > B_c$) regimes. The different phases have distinct subgap signatures in transport, particularly if the depleted S^d region is long enough. In this case, ZBAs appear that are caused by the formation of either a single (in the *topological bulk* phase) or a pair (*topological depletion* phase) of Majorana modes in the junction. The latter is characterized by a residual ZBA splitting. In the case of short junctions, Majoranas cannot develop below B_c , although one may still distinguish between the *conventional* and *minigap* transport regimes (unrelated to Majorana physics) if L_{SO} is large.

Apart from this general analysis, we have discussed a configuration similar to the one in the experiment of Ref. 11. We argue that at least a number of nontrivial features observed in this experiment are consistent with most of our results corresponding to transport through a multimode nonhelical normal/topological depleted superconductor/trivial bulk superconductor junction, hosting Majorana fermion *pairs* within the central region [Figs. 4(d) and 4(e)]. While a qualitative correspondence can be traced between our observations and the experiment, a more quantitative agreement is beyond the goal of our study. This is in part due to a considerable number of unknown parameters (precise L_{SO} , screened gate potential profiles, localization and pair-breaking effects in the bulk superconductor,³⁵ etc.). Moreover, other features that we find, such as the ZBA splitting *oscillations* in B , have not been observed. Thus, a different physical origin of the measured ZBAs (reflectionless tunneling,³⁶ Kondo, etc.) cannot be completely excluded. The latter, however, should be accompanied (at least in its most conventional form) with even-odd effects as a function of gate voltages,³⁷ which are not apparent in Ref. 11. Disorder (not considered here) might also be of relevance. However, its precise role on Majorana physics is currently under active investigation.^{38–40}

Note added in proof. During the review process of our paper, two manuscripts^{41,42} appeared addressing similar questions.

Acknowledgments. We are grateful to S. Frolov and L. Kouwenhoven for fruitful discussions. We acknowledge the support of the CSIC JAE-Doc program and the Spanish Ministry of Science and Innovation through Grants No. FIS2008-00124/FIS (P.S.-J) and No. FIS2009-08744 (E.P. and R.A.). This research was supported in part by the National Science Foundation under Grant No. NSF PHY05-51164.

¹G. Volovik, *JETP Lett.* **70**, 609 (1999).

²N. Read and D. Green, *Phys. Rev. B* **61**, 10267 (2000).

³L. Fu and C. L. Kane, *Phys. Rev. Lett.* **100**, 096407 (2008).

⁴M. Sato, Y. Takahashi, and S. Fujimoto, *Phys. Rev. Lett.* **103**, 020401 (2009).

⁵J. D. Sau, R. M. Lutchyn, S. Tewari, and S. Das Sarma, *Phys. Rev. Lett.* **104**, 040502 (2010).

⁶J. Alicea, *Phys. Rev. B* **81**, 125318 (2010).

⁷R. M. Lutchyn, J. D. Sau, and S. Das Sarma, *Phys. Rev. Lett.* **105**, 077001 (2010).

⁸Y. Oreg, G. Refael, and F. von Oppen, *Phys. Rev. Lett.* **105**, 177002 (2010).

⁹C. W. J. Beenakker, *arXiv:1112.1950v1*.

¹⁰J. Alicea, *Rep. Prog. Phys.* **75**, 076501 (2012).

¹¹V. Mourik, K. Zuo, S. M. Frolov, S. R. Plissard, E. P. A. M. Bakkers, and L. P. Kouwenhoven, *Science* **336**, 1003 (2012).

¹²M. T. Deng, C. L. Yu, G. Y. Huang, M. Larsson, P. Caroff, and H. Q. Xu, *arXiv:1204.4130v1*.

¹³A. Das, Y. Ronen, Y. Most, Y. Oreg, M. Heiblum, and H. Shtrikman, *arXiv:1205.7073v1*.

- ¹⁴K. Sengupta, I. Zutik, H.-J. Kwon, V. M. Yakovenko, and S. Das Sarma, *Phys. Rev. B* **63**, 144531 (2001).
- ¹⁵C. J. Bolech and E. Demler, *Phys. Rev. Lett.* **98**, 237002 (2007).
- ¹⁶K. T. Law, P. A. Lee, and T. K. Ng, *Phys. Rev. Lett.* **103**, 237001 (2009).
- ¹⁷J. D. Sau, S. Tewari, R. M. Lutchyn, T. D. Stanescu, and S. Das Sarma, *Phys. Rev. B* **82**, 214509 (2010).
- ¹⁸T. D. Stanescu, R. M. Lutchyn, and S. Das Sarma, *Phys. Rev. B* **84**, 144522 (2011).
- ¹⁹This gate has turned out to be crucial for the observation of ZBAs in the Delft experiment.
- ²⁰S. Nadj-Perje, V. S. Pribiag, J. W. G. van den Berg, K. Zuo, S. R. Plissard, E. P. A. M. Bakkers, S. M. Frolov, and L. P. Kouwenhoven, *Phys. Rev. Lett.* **108**, 166801 (2012).
- ²¹These parameters, while probably being a good estimation, are not directly measured in the experiment but rather inferred from different samples in a different geometry. Thus significant changes in L_{SO} cannot be excluded.
- ²²G. E. Blonder, M. Tinkham, and T. M. Klapwijk, *Phys. Rev. B* **25**, 4515 (1982).
- ²³See Supplemental Material at <http://link.aps.org/supplemental/10.1103/PhysRevB.86.180503> for a description of the recursive Green's function algorithm for computing transport, including finite width and finite temperature. Also included is an extensive parametric study of differential conductance for varying geometric parameters and spin-orbit lengths, as well as differential conductance maps as a function of bias and depletion gate voltage.
- ²⁴M. Wimmer, A. R. Akhmerov, J. P. Dahlhaus, and C. W. J. Beenakker, *New J. Phys.* **13**, 053016 (2011).
- ²⁵J. D. Sau, C. H. Lin, H.-Y. Hui, and S. Das Sarma, *Phys. Rev. Lett.* **108**, 067001 (2012).
- ²⁶M. Gibertini, F. Taddei, M. Polini, and R. Fazio, *Phys. Rev. B* **85**, 144525 (2012).
- ²⁷D. Chevallier, D. Sticlet, P. Simon, and C. Bena, *Phys. Rev. B* **85**, 235307 (2012).
- ²⁸Note that this structure of the dI/dV remains essentially unchanged in the absence of a depleted region.
- ²⁹M. Cheng, R. M. Lutchyn, V. Galitski, and S. Das Sarma, *Phys. Rev. Lett.* **103**, 107001 (2009).
- ³⁰P. San-Jose, E. Prada, and R. Aguado, *Phys. Rev. Lett.* **108**, 257001 (2012).
- ³¹J. S. Lim, L. Serra, R. Lopez, and R. Aguado, *Phys. Rev. B* **86**, 121103 (2012).
- ³²J. Klinovaja and D. Loss, *Phys. Rev. B* **86**, 085408 (2012).
- ³³Therefore, for single-mode wires, ABSs cannot coexist with the ZBA near zero energy for $B > B_c$. Although this is possible in multimode wires, the ZBA suppression does not occur in such cases.
- ³⁴This is in stark contrast with local probes such as the tunneling current from a metallic tip into the end of the nanowire, see e.g. Ref. 18. Note moreover that a smooth $\Delta(x)$ leaves the dI/dV largely unaffected, which allows us to bypass a self-consistent calculation of the pairing profile.
- ³⁵E. F. C. Driessen, P. C. J. J. Coumou, R. R. Tromp, P. J. de Visser, and T. M. Klapwijk, *Phys. Rev. Lett.* **109**, 107003 (2012).
- ³⁶B. J. van Wees, P. de Vries, P. Magnée, and T. M. Klapwijk, *Phys. Rev. Lett.* **69**, 510 (1992).
- ³⁷E. J. H. Lee, X. Jiang, R. Aguado, G. Katsaros, C. M. Lieber, and S. D. Franceschi, *Phys. Rev. Lett.* **109**, 186802 (2012).
- ³⁸F. Pientka, G. Kells, A. Romito, P. W. Brouwer, and F. von Oppen, [arXiv:1206.0723v1](https://arxiv.org/abs/1206.0723v1) [Phys. Rev. Lett. (to be published)].
- ³⁹D. Bagrets and A. Altland, [arXiv:1206.0434v1](https://arxiv.org/abs/1206.0434v1) [Phys. Rev. Lett. (to be published)].
- ⁴⁰J. Liu, A. C. Potter, K. Law, and P. A. Lee, [arXiv:1206.1276v1](https://arxiv.org/abs/1206.1276v1).
- ⁴¹T. D. Stanescu, S. Tewari, J. D. Sau, and S. Das Sarma, [arXiv:1206.0013](https://arxiv.org/abs/1206.0013).
- ⁴²D. Rainis, L. Trifunovic, J. Klinovaja, and D. Loss, [arXiv:1207.5907](https://arxiv.org/abs/1207.5907).